Electronic Supplementary Information

Stability and Self-passivation of Copper Vanadates under Chemical, Electrochemical, and Photoelectrochemical Operation

Lan Zhou,[a] Qimin Yan,[bc] Jie Yu,[bde] Ryan J. R. Jones,[a] Natalie Becerra-Stasiewicz,[a] Santosh Suram,[a] Aniketa Shinde,[a] Dan Guevarra,[a] Jeffrey B. Neaton,[bcf] Kristin A. Persson,[*e] and John M. Gregoire[*a]

[a] Joint Center for Artificial Photosynthesis, California Institute of Technology, Pasadena, CA 91125, USA.
Email: gregoire@caltech.edu
[b] Molecular Foundry, Lawrence Berkeley National Laboratory, Berkeley, CA 94720, USA.
[c] Department of Physics, University of California, Berkeley, CA 94720, USA.
[d] Joint Center for Artificial Photosynthesis, Lawrence Berkeley National Laboratory, Berkeley, CA 94720, USA.
[e] Environmental Energy Technologies Division, Lawrence Berkeley National Laboratory, Berkeley, CA 94720, USA.
Email: kapersson@lbl.gov
[f] Kavli Energy NanoSciences Institute, Berkeley, CA 94720, USA.

Library synthesis

Three Cu-V oxide composition libraries were fabricated using reactive RF magnetron co-sputtering of Cu and V metal targets onto 2 different types of substrates. A summary of the 3 libraries and the composition stability measurement techniques is provided in Table 1. Library A was deposited onto a 10 cm-diameter Si wafer with more than 100 nm of thermal oxide, which served as a diffusion barrier. Libraries B and C were deposited on 10 cm-diameter glass substrates with a fluorine doped tin oxide (FTO) coating (Tec7, Hartford Glass Company). All depositions proceeded in a combinatorial sputtering system (Kurt J. Lesker, CMS24) with 10^{-5} Pa base pressure. The deposition atmosphere was composed of inert sputtering gas Ar (0.72 Pa) and reactive gas O_2 (0.08 Pa). The composition gradients in the co-sputtered continuous composition spreads were attained by positioning the deposition sources in a non-confocal geometry.[1] All depositions proceeded for about 20 hours with no intentional substrate heating, with the power on the V source at 150 W and with the power on the Cu source at 25 W, 12 W and 15 W for libraries A, B and C, respectively. The as-deposited composition libraries were subsequently annealed in a Thermo Scientific box oven in flowing air at 610 °C for 1 hour (library A) or at 550 °C for 3 hours (libraries B and C). The annealing was preceded by a 2 hour temperature ramp and was followed by natural cooling. Since the oxygen stoichiometry is not specifically controlled or measured, we refer to the post-anneal library compositions as $Cu_{1-x}V_xO_z$, where z is expected to be approximately $1 + 1.5\ x$. This assumption is in agreement with previously reported and present film characterization in which each thin film composition crystallizes into oxide structures comprised of Cu^{2+} and V^{5+}.[2] The film thickness was not measured for each library or composition sample but was estimated to be 400 nm based on deposition rate calibrations from the Cu and V sputter sources.

Table S1. Summary of 3 composition libraries and the composition stability measurements

Library	x in $Cu_{1-x}V_xO_z$	Annealing Temperature	Composition Techniques	Stability Process
A	0.12 – 0.67	610°C, 1 hr	XRF, XPS	Chemical
B	0.24 – 0.67	550°C, 3 hr	XRF	Electrochemical
C	0.29 – 0.47	550°C, 3 hr	EDS, XPS	Photoelectrochemical

X-ray diffraction

The crystal structures and phase distribution of the composition libraries were determined through x-ray diffraction (XRD) measurements with the x-ray spot size limited to a 1 mm length scale, over which the composition is constant to within approximately 1%. For the $Cu_{1-x}V_xO_z$ libraries, a series of measurements across the composition gradient was used to generate a structural phase map to elucidate structure-property relationships.

The high throughput XRD experiment on library A was conducted using a combinatorial scattering experiment incorporated into the bending magnet beam line 1-5 at SSRL, as described previously.[3] Briefly, a Si (111) double crystal monochromator provided a 13 keV x-ray beam (wavelength 0.0954 nm), which after slitting to 1 × 0.1 mm cross section contained a photon flux of approximately 10^{11} photons s^{-1}. The substrate with composition library was tilted such that substrate normal was 84° from the beam, providing a footprint of approximately 1 × 1 mm on the sample. X-ray scattering images were acquired in reflection geometry with a Princeton Quad-RO 4320 with fiber optic-coupled CCD chip, and an integration time of 45 s was used for each of the 11 composition samples. Calibration of the scattering geometry using a LaB_6 powder, and subsequent integration of the scattering images to one-dimensional XRD patterns (intensity vs. scattering vector magnitude) was performed using WxDiff software.

XRD experiments on libraries B and C were performed using a Bruker DISCOVER D8 diffractometer with Cu K_α radiation from a Bruker IμS source (Bruker AXS Inc., Madison, WI). Using a 0.5 mm collimator, the effective thin film measurement area was approximately 0.5 × 1 mm. Diffraction images were collected using a two-dimensional VÅNTEC-500 detector and integrated into one-dimensional patterns using DIFFRAC.SUITE™ EVA software. For patterns in which multiple crystalline phases were identified, the relative phase fraction of each phase was approximated by normalizing the measured intensity of the most distinguishing peak of each phase.

To establish composition-structure-stability measurements, the phase behavior of each library was assessed from the series of XRD measurements. For library A, the high throughput synchrotron XRD data for the full composition library is shown in Fig. S1a with a representative pattern and phase identification shown in Fig. S1b. The datasets for libraries B and C were similarly analyzed, requiring more diligent manual inspection due to the strong signal from the FTO coating, as previously discussed.[2] Examples of XRD patterns at the phase pure regions in library C deposited on FTO glass are shown in Fig. S2.

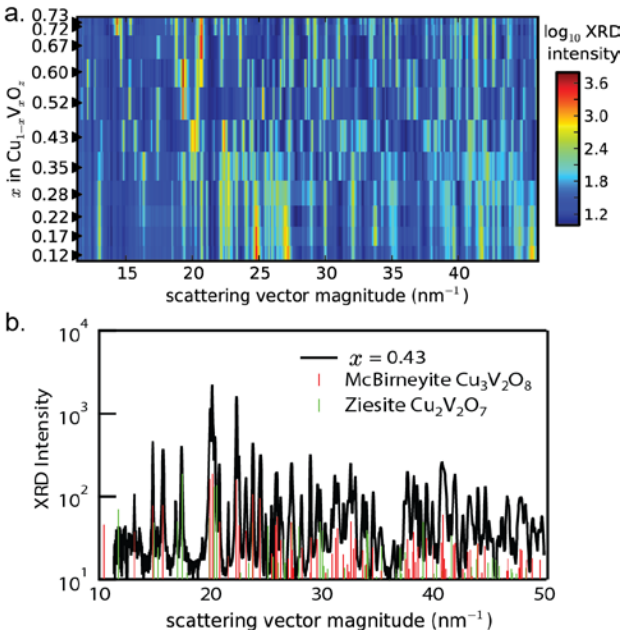

Fig. S1 a) 2D XRD mapping of $Cu_{1-x}V_xO_z$ using library A, and b) a representative XRD pattern at x = 0.43, where shows the mixed phases of γ-$Cu_3V_2O_8$ (McBirneyite) and β-$Cu_2V_2O_7$ (Ziesite).

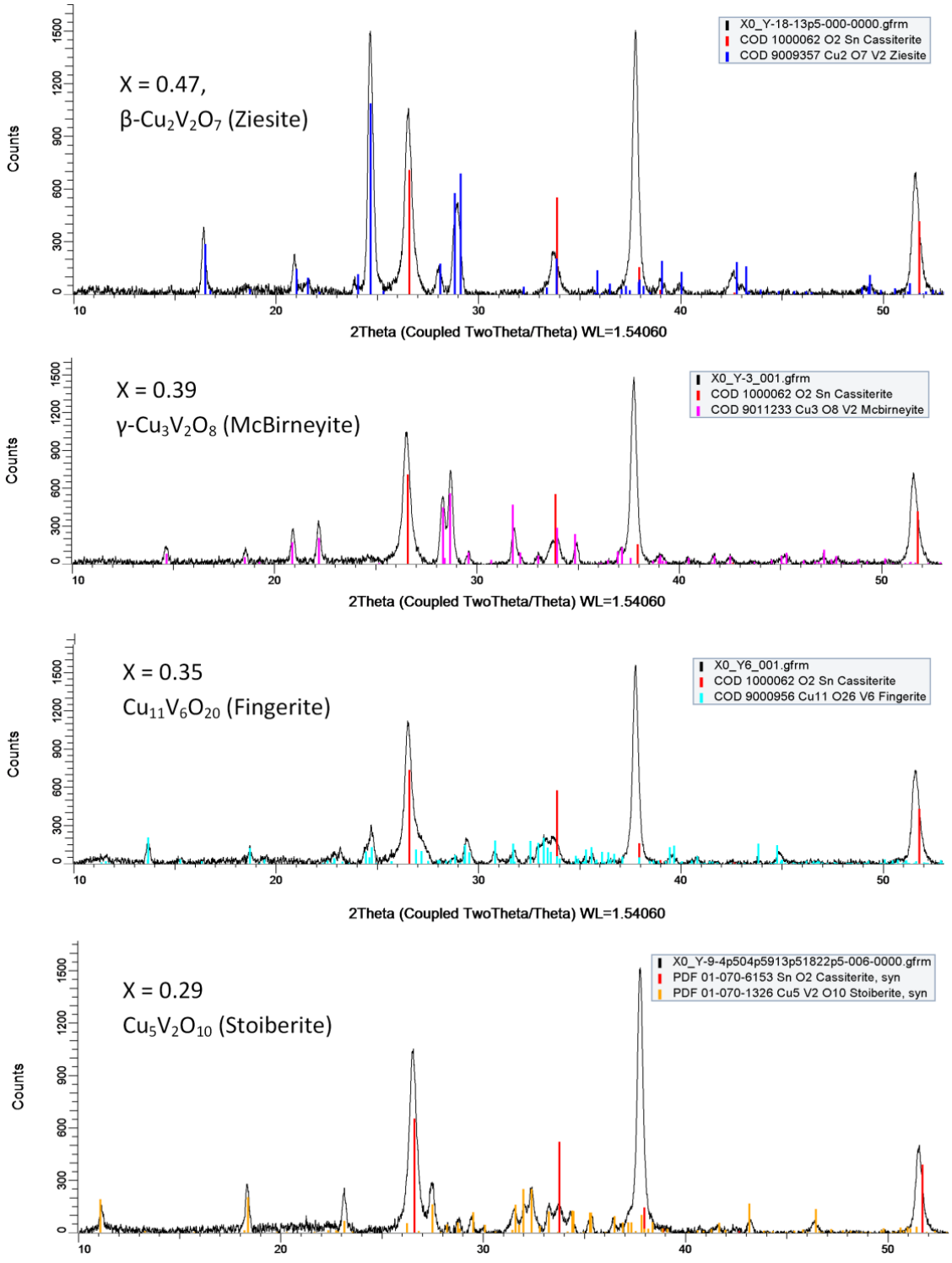

Fig. S2 XRD patterns of pure β-$Cu_2V_2O_7$ (Ziesite), γ-$Cu_3V_2O_8$ (McBirneyite), $Cu_{11}V_6O_{26}$ (Fingerite) and $Cu_5V_2O_{10}$ (Stoiberite) phases in library C. The red stick pattern shows the strong signal from FTO layer.

Composition measurements

A suite of 3 thin film measurement techniques were employed to measure the composition of the thin films library both as-prepared and post-stability experiment. To quantify the thickness-averaged Cu:V composition of each thin film sample (so-called "bulk" composition), x-ray fluorescence (XRF) measurements were performed on libraries A and B, and energy-dispersive x-ray spectroscopy (EDS) measurements were performed on library C. The XRF measurements were performed on an EDAX Orbis Micro-XRF system (EDAX Inc., Mahwah, NJ) with an x-ray beam approximately 1 mm in diameter. The EDS measurements were performed using an Oxford Instruments X-Max (Oxford Instruments, Concord, MA) detector on a FEI Nova NanoSEM 450 (FEI, Hillsboro, OR) with excitation from a 12 keV electron beam. For both XRF and EDS measurements, the Cu K and V K fluorescent x-rays were used for elemental quantification, and the escape depth of these x-rays, as well as the penetration depth of the XRF x-rays and EDS electron source, are beyond the thickness of the $Cu_{1-x}V_xO_z$ thin films. The EDS composition quantification was performed using a thin film model in the INCAEnergy EDS analysis software, and while no thin film modelling was applied to the XRF composition quantification, comparisons between XRF and EDS measurements showed agreement within the typical 5-10% uncertainty of standardless composition quantification.

The near-surface composition of select composition samples was measured by x-ray photoelectron spectroscopy (XPS) using a Kratos Axis NOVA (Kratos Analytical, Manchester, UK) with excitation from a monochromatized Al K_α (1486.6 eV) at 300 W (20 mA at 15 kV). The measurement area was approximately 0.8 mm in diameter with a take-off angle to the detector of 35.5°. Pressure in the surface analysis chamber was low 10^{-7} Pa during the measurements. Survey spectra were collected at pass energy 160 eV with a step size of 0.05 eV, and high-resolution scans at pass energy 10 eV with a step size of 0.025 eV. The measurements were performed without active charge neutralization, but no substantial sample charging was observed. Sample-specific binding energy shifts on the order of 1 eV were observed, and for each measurement sample, the binding energy was calibrated to the survey scan C 1s peak position of 284.8 eV. Elemental quantification was performed in the CasaXPS software using a Shirley background fitting of the Cu $2p_{3/2}$ and V $2p_{3/2}$ peaks in the survey scans. To calculate the Cu:V composition, database relative sensitivity factors (R.S.F.) of 3.547 and 1.411 were used for Cu $2p_{3/2}$ and V $2p_{3/2}$ peaks, respectively.[4]

The XRD, EDS and XPS compositions are reported as the V concentration *x* in $Cu_{1-x}V_xO_z$, and we note that while absolute uncertainty is typically 5-10% for these measurements, the relative measurements within a composition library have better than 5% accuracy. We find that the absolute XRF counts for a given element are reproducible to within 5%, which enables quantitative comparison of as-prepared and post-experiment elemental XRF signals. The XRF and EDS measurements of the as-prepared composition of each library provide a baseline against which the near-surface (XPS) composition and post-stability experiment compositions can be compared. Fig. S3 shows an example pair of XRF spectra for the x = 0.30 composition sample of library B. The spectra show the V K and Cu K alpha peaks used for composition quantification as well as signals from the FTO layer (Sn), glass substrate (Si, Fe) and x-ray source (Rh). This figure also shows that the XRF spectrum of this sample remains remarkably unchanged by the 2 hour electrochemical experiment.

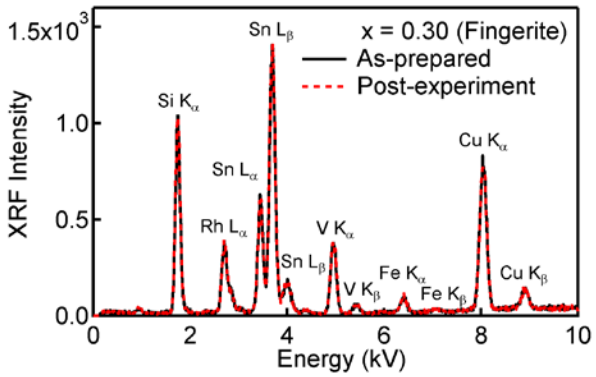

Fig. S3 XRF spectra for the *x* = 0.30 composition sample (pure $Cu_{11}V_6O_{26}$-Fingerite region indicated by XRD) from library B before and after 2 hour electrochemical stability measurement in pH 9.2 at the OER equilibrium potential $E_{H2O/O2}$ (1.23 V vs. RHE).

Since XPS experiments are relatively resource intensive, these measurements were performed on a smaller set of compositions in libraries A and C. Here we discuss the x = 0.39 sample from library C, which was determined to be phase pure γ-$Cu_3V_2O_8$ (McBirneyite) in the XRD measurements, and note that it is representative of the XPS measurements on the 9 as-prepared and 7 post-experiment samples. Figure 4 in the main text shows the survey spectra and high-resolution core level XPS spectra of γ-$Cu_3V_2O_8$ before and after the 40 min PEC stability measurement. The values of the photoelectron binding energy were calibrated using the C 1s peak at 284.8 eV, as shown in Fig. 4b, as the internal standard. While adhered drops of electrolyte were removed from the sample during its extraction from the PEC cell, small signals from electrolyte-constituent elements K and B are apparent in the post-experiment survey spectrum. We have not determined whether these elements are present as precipitated salts and if their surface coverage is uniform or sparse. The C 1s peak is also more intense in the post-experiment spectrum, and since the surface was not cleaned prior to XPS measurements, these coatings may have minor effects on the calculated Cu:V composition, which we ignore for the purposes of the present work.

A detailed analysis of XPS spectra of Cu and V oxides is provided by Biesinger et al.,[5] and the interpretation of Cu 2p and V 2p XPS signals was performed with respect to the data in this reference. As noted above, all of the observed copper vanadate phases are comprised of Cu^{2+} and V^{5+} cations. Correspondingly, the V 2p core level spectrum from the as-prepared film (Fig. 4d) contains well-defined spin-orbit doublet peaks at 517.1 eV and 524.7 eV, in reasonable agreement with the literature values of 517.26 eV and 524.74 eV for pentavalent V $2p_{3/2}$ and V $2p_{1/2}$, respectively. In Fig. 4c, the Cu 2p spin-orbit doublet peaks at 934.5 eV and 954.4 eV are slightly larger than the literature binding energies of 933.57 eV and 953.52 eV for Cu 2p in CuO. The presence and shape of the strong satellite peaks are in excellent agreement with the literature CuO spectrum; the Cu 2p signal from Cu_2O has much less pronounced satellite peaks. In Fig. 4c the Cu $2p_{3/2}$ peak exhibits a small shoulder peak at lower binding energy, which is likely due to the presence of a small fraction of Cu^{1+}, indicating that the surface of γ-$Cu_3V_2O_8$ phase can be reducible in ambient air or XPS high vacuum conditions. A similar Cu 2p signal was observed on all XPS measurements of copper vanadate phases, with the β-$Cu_2V_2O_7$ phase exhibiting the strongest Cu^{1+} signal, as shown in Fig. S4.

As shown in Fig. 3c, Cu 2p spectra remain largely unchanged by the 40 min PEC operation, except the decrease in intensity for the Cu $2p_{3/2}$ peak and a slight shift to lower binding energy, from 934.5 eV to 934.2 eV. The V 2p spectra show a relatively large decrease in signal intensity, indicating a substantial loss of V in the near-surface region. Moreover, the V 2p doublet peaks shift to 516.4 eV and 523.9 eV, which are a closer match to the published values for VO_2. As shown in the O 1s signal in Fig. 4d, the post-experiment spectrum exhibits a decreased intensity of the 529.9 eV peak observed in the as-prepared film, and a new peak at 531.2 eV is observed, which may be due to the formation of a metal hydroxide(s) during operation in the alkaline electrolyte. The compilation of these observations reveals that the near-surface region is certainly modified by the PEC experiment. The Cu is mostly retained and remains predominantly in a Cu^{2+}-like state in a near-surface layer that contains V and O with the possible complexation of K and B species from the electrolyte. This detailed analysis of the XPS data indicates the formation of a Cu-rich protective coating on the γ-$Cu_3V_2O_8$ sample during PEC operation.

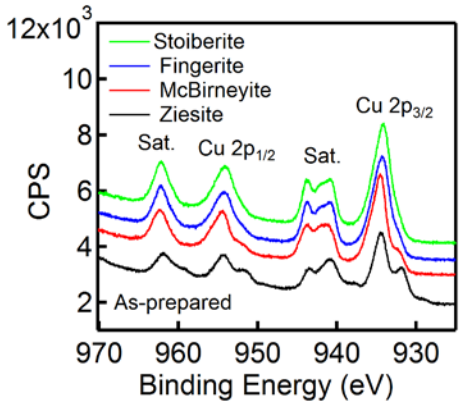

Fig. S4 High-resolution Cu 2p core-level XPS spectra of as-prepared $Cu_5V_2O_{10}$ (Stoiberite), $Cu_{11}V_6O_{26}$ (Fingerite), γ-$Cu_3V_2O_8$ (McBirneyite), and β-$Cu_2V_2O_7$ (Ziesite) phases in library C, respectively. The spectra were shifted vertically for clarity.

Chemical, electrochemical and photoelectrochemical experiments on libraries A, B and C

To evaluate composition stability of various $Cu_{1-x}V_xO_z$ compositions and phases, chemical, electrochemical and PEC experiments were performed on libraries A, B and C, respectively. All experiments were performed in an aqueous electrolyte solution of 0.1 M boric acid with approximately 0.05 M potassium hydroxide, resulting in an electrolyte solution buffered at pH 9.2. The chemical experiment (library A) proceeded by soaking a 1 × 10 cm strip of Si substrate with the composition library in 1 L of solution for 48 hours. Upon extraction of the library, it was placed film-side down on a lab wipe to absorb the wetted solution.

The electrochemical experiment (library B) was performed on the entire 10 cm-diameter composition library using a recently-developed parallel electrochemical treatment system.[6] Using an o-ring seal with inner diameter of 8.4 cm, the corresponding area of composition library was exposed to a uniform electrochemical environment for 2 hours. Cu tape was applied to the FTO layer to make electrical contact to the composition library, which served as the working electrode, and a planar stainless steel mesh counter electrode was suspended parallel to the working electrode with an inter-planar spacing of approximately 10 mm. A reference electrode (Ag/AgCl, CH Instruments) was placed less than 5 mm from the plane of the working electrode surface to establish a pseudo 3-electrode cell. A sheet of porous polypropylene (PP) with pore size 80 – 155 micron (Porex) separated the working and reference electrode (anolyte chamber) from the counter electrode (catholyte chamber) and continuous flow of the electrolyte was maintained at approximately 10 mL min^{-1} in both the anolyte and catholyte chambers with separate 1 L electrolyte reservoirs. The PP frit and electrolyte flow mitigated any cross-over of reaction products from the counter electrode to the working electrode and vice versa. A constant potential of 1.23 V vs. RHE was applied for the 2 hour duration of the electrochemical experiment.

It is worth noting that electrochemical stability can be promoted through the establishment of a high concentration of metal species in solution, for example in so-called self-healing catalysts.[7] To ensure that the composition stability measurements were performed in the aggressive conditions of sub-1 μM concentrations of Cu and V species, large electrolyte volumes were employed for the long-duration chemical and electrochemical experiments. The shorter-duration PEC experiment used a smaller electrolyte volume due to constraints of the illumination apparatus and PEC cell.

The photoelectrochemical experiment (library C) was performed in a rectangular polycarbonate cell in which one wall was replaced by a quartz window (GM Associates, Inc., Oakland, CA), which provided optical access into the PEC cell. The incident light source was an ABET Sun 3000 AAA solar simulator with an AM 1.5G filter. The incident light spectrum was confirmed to conform to AM 1.5G using a Black Comet spectrometer (StellarNet, Inc., Tampa, FL) with incident light intensity set at 100 mW cm^{-2} using a silicon reference cell (ABET) and a silicon photodiode (Thorlabs, Inc., Newton, NJ). A 1 cm-wide strip of library C was cut from the glass substrate and mounted in a custom holder which made electrical contact to the library and to a planar Ni foil counter electrode mounted approximately 2 mm from the substrate. As in the electrochemical cell, a Ag/AgCl reference electrode was placed between the working and counter electrodes. The 3-electrode assembly was prepared out of the PEC cell, and before the experiment commenced, the 1.23 V vs. RHE voltage was applied to the working electrode and the calibrated AM 1.5G source was applied to illuminate the entire cell. Under potential control, the library was lowered into the cell with back-side illumination of the composition library and remained under PEC control for 40 minutes. A magnetic stir bar provided continual electrolyte convection between the working and counter electrodes. The working electrode was removed from the electrolyte solution under PEC control and a dry N_2 stream was applied to the surface of the library as it was gradually removed to blow away wetted drops of solution and mitigate precipitation of salts onto the composition library.

During the potentiostatic electrochemical and PEC measurements, the current provided by the entire composition library was measured, but the parallel nature of these experiments preclude a direct relationship between the electrochemical current and specific library compositions. For the 2 hour electrochemical experiment (library B), no OER electrocatalysis could occur due to the application of the Nernstian OER potential, and given the finding that the majority of the library remained compositionally stable, the current should be near zero. Indeed, an anodic current of less than 3 μA for the entire 55.4 cm^2 electrode was observed for most of the 2 hour experiment. For the PEC experiment (library C), the AM 1.5 illumination enables photoelectrocatalysis of the OER. Estimating an expected PEC current is difficult given our recently-reported composition and structure maps of the OER photocurrent of similar composition libraries, in which the photocurrent was quite sensitive to both composition and structure.[2] That is, maxima in photocurrent were observed at nearly-phase-pure regions of the library. The 40 min photocurrent measurement is shown in Fig. S5, demonstrating that the photocurrent from the 5 cm^2 electrode dropped from approximately 1 mA to 20 μA over the first 10 minutes and then remained relatively stable thereafter. This rapid initial

decay in the photocurrent is indicative of photo-corrosion or another deactivation process. Given the model of a Cu-rich passivation layer, these results indicate that the formation of the protective, non-stoichiometric surface layer self-passivates the photoanodes from bulk corrosion but degrades the photoelectrocatalytic activity of these materials. The photocurrent signal is unexpectedly low, leading to the investigation of illumination-dependent stability is in the following section.

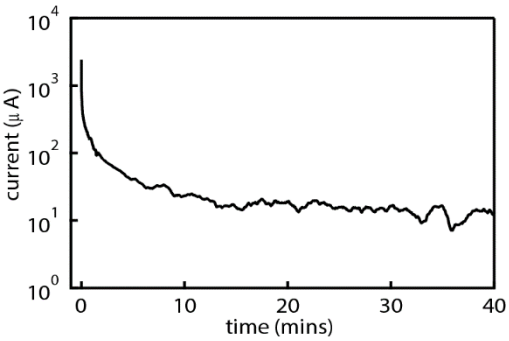

Fig. S5 Photocurrent evolution during 40 min photoelectrochemical experiment on a 1-cm wide strip of Library C in pH 9.2 at 1.23 V vs RHE.

Additional photoelectrochemical characterization and illumination-dependent stability

Additional photoelectrochemical measurements were performed on duplicate samples using a scanning droplet cell (SDC)[8] with illumination from either a 385 nm LED or Xe lamp with IR filter. A chopped-illumination CV of the γ-$Cu_3V_2O_8$ samples with the LED illumination is shown in Figure S6, demonstrating excellent performance and stability. To assess longer-term stability, a 30 minute chopped-illumination measurement at 1.23 V vs RHE is shown in Figure S7. The photocurrent remained between 0.26 and 0.29 mA cm^{-2} for the duration of the measurement, indicating near-perfect stability in stark contrast to the photocurrent measurement in Fig. S5. The illumination from the xenon lamp provided an irradiance of approximately 297 mW cm^{-2} in the UV-visible range of 380-1000 nm, approximately 4.7 times larger than that of AM 1.5G. The xenon lamp spectrum was filtered with a Newport 6123NS to remove all infrared radiation with wavelength above approximately 1200 nm. In the 380-1000 nm range, the ABET solar simulator yielded approximately 1.05 times the AM 1.5G irradiance for the PEC measurement of library C. This lamp has no infrared filter and due to the thin cell used for the measurement, the infrared irradiance on the sample likely resulted in a substantial temperature rise. While the temperature was not measured during this experiment, similar measurements using this light source yielded cell temperatures in excess of 50 ^{o}C. A calibrated spectrometer was used to measure the spectral irradiance from the Xe lamp used for the SDC measurements with solution present and the ABET lamp used for the PEC measurement of library C at the sample location but without solution present. The spectra are shown along with the AM 1.5G spectrum in Figure S8.

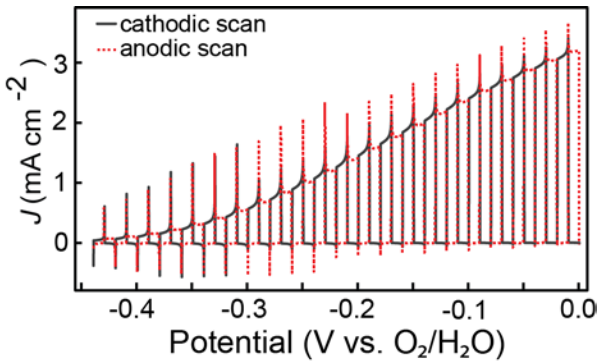

Fig. S6 Chopped-illumination CV of γ-$Cu_3V_2O_8$ with UV (385 nm LED) illumination in pH 9.2.

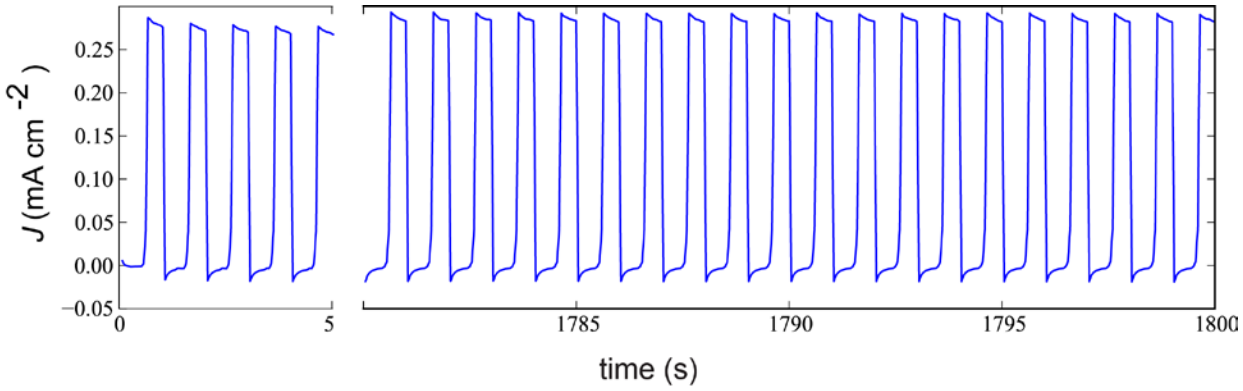

Fig. S7 Chopped-illumination photocurrent of γ-$Cu_3V_2O_8$ in pH 9.2 at 1.23 V vs RHE with approximately 4-suns illumination in the UV-visible but no infrared illumination. The first 5 and last 20 illumination cycles are shown, demonstrating excellent stability compare to that observed in Fig S5.

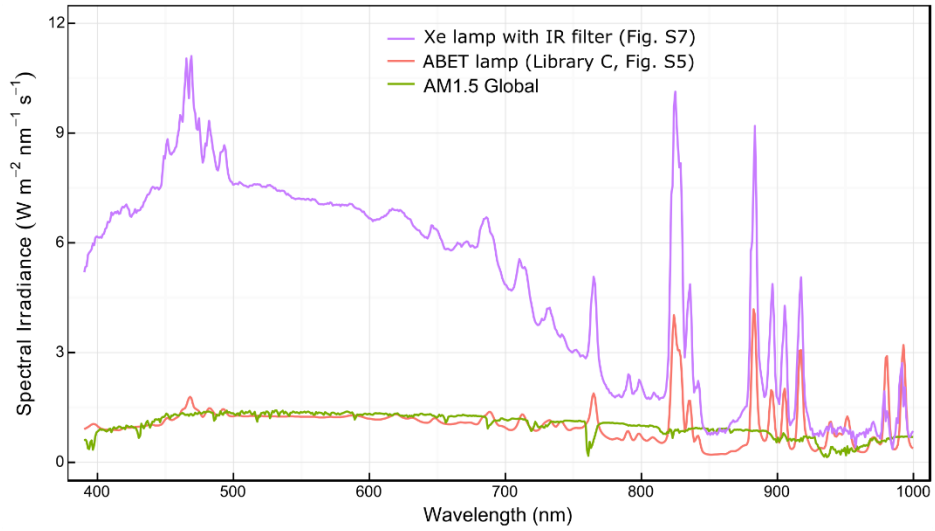

Fig. S8 Lamp spectra for the photoelectrochemical measurement on Library C with simulated AM 1.5G (Fig. S5) and on γ-$Cu_3V_2O_8$ with concentrated UV-visible and filtered IR irradiance (Fig. S7). The AM 1.5G spectrum is shown for comparison.

To compare stability among the measurements in the present work and those previously reported, Table 1 shows photocurrent data for 4 copper vanadate phases and the phase mixture of Library C in pH 9.2 borate-buffered electrolyte at potentials between 1.23-1.6 V vs RHE. The measured 380-1000 nm irradiance in the present work and our measured 385 nm LED irradiance are shown, and for reports from other groups the nominal irradiance assuming a AM 1.5G spectrum is shown. The solar simulator experiment with strong infrared irradiation is colored red and is the only experiment that shows substantial degradation in photocurrent over 30-180 minute-duration experiments. Our experiments with no infrared irradiation are colored grey and show excellent stability. Reports from other groups with unknown infrared irradiation (no report of calibration in the infrared or illumination distance through aqueous electrolyte, which filters infrared radiation) are colored cyan and also show excellent stability. The suggestion of these results is that all of the copper vanadate photoelectrocatalysts reported to date are quite stable in pH 9.2 borate-buffered electrolyte as long as the material is not heated through strong infrared radiation. It is important to note that even when the photocurrent degrades, as in Fig S5, the photocurrent is still finite and the copper vanadates still self-passivate.

Table S2. Summary of photoelectrochemical stability measurements in pH 9.2 electrolytes with rows colored according to no illumination (no color), AM 1.5G with strong infrared radiation (red), illumination with infrared filter or only UV illumination (grey), and nominal AM 1.5G illumination with unknown infrared radiation (cyan).

phase	Potential V vs RHE	Illumination description	Irradiance 380-1000 nm, mW cm^{-2}	J at t~0, mA cm^{-2}	J later, mA cm^{-2}	time later, mins	reference
Mixed (library C)	1.23	None (dark)	0	<0.01	<0.01	120	This work
Mixed (library C)	1.23	ABET Sun 3000 AAA, 1.5G filter	66	2.4	0.01	40	This work
γ-$Cu_3V_2O_8$	1.23	450 W Xe lamp with IR filter	297	0.27	0.28	30	This work
γ-$Cu_3V_2O_8$	1.23	385 nm LED	170	1.8	1.75	30	Zhou et.al.[9]
α-$Cu_2V_2O_7$	1.23	385 nm LED	170	1.7	1.55	30	Zhou et.al.[9]
β-$Cu_2V_2O_7$	1.23	385 nm LED	170	2.0	1.6	30	Zhou et.al.[9]
β-$Cu_3V_2O_8$	1.6	300 W Xe, calibrated above 2 eV to 1 sun	Nominally 63	0.027	0.027	30	Seabold et. al.[10]
α-CuV_2O_6	1.58	150 W Xe lamp, AM 1.5G filter	Nominally 63	0.21	0.19	180	Guo et. al.[11]
β-$Cu_2V_2O_7$	1.58	150 W Xe lamp, AM 1.5G filter	Nominally 63	0.125	0.125	180	Guo et. al.[11]

References

1. Suram, S. K.; Zhou, L.; Becerra-Stasiewicz, N.; Kan, K.; Jones, R. J. R.; Kendrick, B. M.; Gregoire, J. M., Combinatorial thin film composition mapping using three dimensional deposition profiles. *Rev. Sci. Instrum.* **2015,** *86*, 033904.
2. Zhou, L.; Yan, Q.; Shinde, A.; Guevarra, D.; Newhouse, P. F.; Becerra-Stasiewicz, N.; Chatman, S. M.; Haber, J. A.; Neaton, J. B.; Gregoire, J. M., High Throughput Discovery of Solar Fuels Photoanodes in the CuO–V_2O_5 System. *Adv. Energy Mater.* **2015**, n/a-n/a.
3. Gregoire, J. M.; Van Campen, D. G.; Miller, C. E.; Jones, R.; Suram, S. K.; A., M., High Throughput Synchrotron X-ray Diffraction for Combinatorial Phase Mapping. *J. Synchrotron Radiat.* **2014,** *21* (6), 1262-1268.
4. Wagner, C. D.; Naumkin, A. V.; Kraut-Vass, A.; Allison, J. W.; Powell; C.J.; Rumble Jr., J. R., NIST Standard Reference Database 20. 2003; Vol. Version 3.4 (web version)
5. Biesinger, M. C.; Lau, L. W. M.; Gerson, A. R.; Smart, R. S. C., Resolving surface chemical states in XPS analysis of first row transition metals, oxides and hydroxides: Sc, Ti, V, Cu and Zn. *Appl. Surf. Sci.* **2010,** *257* (3), 887-898.
6. (a) Shinde, A.; Jones, R. J. R.; Guevarra, D.; Mitrovic, S.; Becerra-Stasiewicz, N.; Haber, J. a.; Jin, J.; Gregoire, J. M., High-Throughput Screening for Acid-Stable Oxygen Evolution Electrocatalysts in the (Mn–Co–Ta–Sb)O x Composition Space. *Electrocatalysis* **2015,** *6* (2), 229-236; (b) Jones, R. J. R.; Shinde, A.; Guevarra, D.; Xiang, C.; Haber, J. a.; Jin, J.; Gregoire, J. M., Parallel electrochemical treatment system and application for identifying Acid-stable oxygen evolution electrocatalysts. *ACS Combinatorial Science* **2015,** *17* (2), 71-5.
7. Bediako, D. K.; Ullman, A. M.; Nocera, D. G., Catalytic Oxygen Evolution by Cobalt Oxido Thin Films. *Topics in current chemistry* **2016,** *371*, 173-213.

8. Gregoire, J. M.; Xiang, C.; Liu, X.; Marcin, M.; Jin, J., Scanning Droplet Cell for High Throughput Electrochemical and Photoelectrochemical Measurements. *Rev. Sci. Instrum.* **2013,** *84* (2), 024102.
9. Zhou, L.; Yan, Q.; Shinde, A.; Guevarra, D.; Newhouse, P. F.; Becerra-Stasiewicz, N.; Chatman, S. M.; Haber, J. A.; Neaton, J. B.; Gregoire, J. M., High Throughput Discovery of Solar Fuels Photoanodes in the CuO–V2O5 System. *Adv. Energy Mater.* **2015,** *5*, 1500968.
10. Seabold, J. A.; Neale, N. R., All First Row Transition Metal Oxide Photoanode for Water Splitting Based on Cu3V2O8. *Chemistry of Materials* **2015,** *27* (3), 1005-1013.
11. Guo, W.; Chemelewski, W. D.; Mabayoje, O.; Xiao, P.; Zhang, Y.; Mullins, C. B., Synthesis and Characterization of CuV2O6 and Cu2V2O7: Two Photoanode Candidates for Photoelectrochemical Water Oxidation. *The Journal of Physical Chemistry C* **2015,** *119* (49), 27220-27227.